

IMPROVED CATHODE COMPOSITIONS FOR LITHIUM-ION BATTERIES

TECHNICAL FIELD

This invention relates to preparing compositions useful as cathodes for lithium-ion batteries.

BACKGROUND

5 Lithium-ion batteries typically include an anode, an electrolyte, and a cathode that contains lithium in the form of a lithium-transition metal oxide. Examples of transition metal oxides that have been used include cobalt dioxide, nickel dioxide, and manganese dioxide. None of these materials, however, exhibits an optimal combination of high initial capacity, high thermal stability, and good capacity retention after repeated charge-discharge cycling.

SUMMARY

10 In general, the invention features a cathode composition for a lithium-ion battery having the formula $\text{Li}[\text{M}^1_{(1-x)}\text{Mn}_x]\text{O}_2$ where $0 < x < 1$ and M^1 represents one or more metal elements, with the proviso that M^1 is a metal element other than chromium. The composition is in the form of a single phase having an O3 crystal structure that does not undergo a phase transformation to a spinel crystal structure when incorporated in a lithium-ion battery and
15 cycled for 100 full charge-discharge cycles at 30°C and a final capacity of 130 mAh/g using a discharge current of 30 mA/g. The invention also features lithium-ion batteries incorporating these cathode compositions in combination with an anode and an electrolyte.

20 In one embodiment, $x = (2-y)/3$ and $\text{M}^1_{(1-x)}$ has the formula $\text{Li}_{(1-2y)/3}\text{M}^2_y$, where $0 < y < 0.5$ (preferably $0.083 < y < 0.5$, and more preferably $0.167 < y < 0.5$) and M^2 represents one or more metal elements, with the proviso that M^2 is a metal element other than chromium. The resulting cathode composition has the formula $\text{Li}[\text{Li}_{(1-2y)/3}\text{M}^2_y\text{Mn}_{(2-y)/3}]\text{O}_2$.

In a second embodiment, $x = (2-2y)/3$ and $\text{M}^1_{(1-x)}$ has the formula $\text{Li}_{(1-y)/3}\text{M}^3_y$, where $0 < y < 0.5$ (preferably $0.083 < y < 0.5$, and more preferably $0.167 < y < 0.5$) and M^3 represents one or

more metal elements, with the proviso that M^3 is a metal element other than chromium. The resulting cathode composition has the formula $Li[Li_{(1-y)/3}M^3_yMn_{(2-2y)/3}]O_2$.

In a third embodiment, $x = y$ and $M^1_{(1-x)}$ has the formula $M^4_yM^5_{1-2y}$, where $0 < y < 0.5$ (preferably $0.083 < y < 0.5$, and more preferably $0.167 < y < 0.5$), M^4 is a metal element other than chromium, and M^5 is a metal element other than chromium and different from M^4 . The resulting cathode composition has the formula $Li[M^4_yM^5_{1-2y}Mn_y]O_2$.

The invention provides cathode compositions, and lithium-ion batteries incorporating these compositions, that exhibit high initial capacities and good capacity retention after repeated charge-discharge cycling. In addition, the cathode compositions do not evolve substantial amounts of heat during elevated temperature abuse, thereby improving battery safety.

The details of one or more embodiments of the invention are set forth in the accompanying drawings and the description below. Other features, objects, and advantages of the invention will be apparent from the description and drawings, and from the claims.

DESCRIPTION OF DRAWINGS

FIG. 1 is an exploded perspective view of an electrochemical cell used to test various electrode compositions.

FIGS. 2(a)-(e) are plots of voltage versus capacity and capacity versus cycle number for the samples described in Examples 1 and 3-6 cycled between 4.4 V and 3.0 V.

FIGS. 3(a)-(e) are plots of voltage versus capacity and capacity versus cycle number for the samples described in Examples 1 and 3-6 cycled between 4.8 V and 2.0 V.

FIGS. 4(a)-(d) are x-ray diffraction patterns for the samples described in Examples 3 and 7-9.

FIGS. 5(a)-(d) are x-ray diffraction patterns for the samples described in Examples 5 and 10-12.

FIGS. 6(a)-(d) are x-ray diffraction patterns for the samples described in Examples 6 and 16-18.

FIGS. 7(a)-(d) are plots of voltage versus capacity and capacity versus cycle number for the samples described in Examples 6 and 16-18 cycled between 4.4 V and 3.0 V.

FIGS. 8(a)-(d) are plots of voltage versus capacity and capacity versus cycle number for the samples described in Examples 6 and 16-18 cycled between 4.8 V and 2.0 V.

FIGS. 9(a)-(b) are plots of voltage versus capacity for the samples described in Examples 19 and 20.

FIG. 10 is a plot of capacity versus cycle number for the sample described in Example 19 cycled between 4.4V and 2.5 V.

Fig. 11 is a plot of capacity versus cycle number for the sample described in Example 20 cycled between 4.4 V and 2.5 V.

Fig. 12 is a plot of capacity versus cycle number for the sample described in Example 1 cycled between 4.4 V and 3.0 V at both 30°C and 55°C.

Fig. 13 is a plot of capacity versus discharge current density for the sample described in Example 1 measured at 30°C to a 2.5 V cutoff.

DETAILED DESCRIPTION

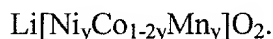
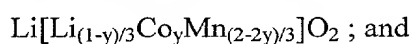
Cathode compositions have the formulae set forth in the Summary of the Invention, above. The formulae themselves, as well as the choice of particular metal elements, and combinations thereof, for $M^1 - M^5$, reflect certain criteria that the inventors have discovered are useful for maximizing cathode performance. First, the cathode compositions preferably adopt an O3 crystal structure featuring layers generally arranged in the sequence lithium-oxygen-metal-oxygen-lithium. This crystal structure is retained when the cathode composition is incorporated in a lithium-ion battery and cycled for 100 full charge-discharge cycles at 30°C and a final capacity of 130 mAh/g using a discharge current of 30 mA/g, rather than transforming into a spinel-type crystal structure under these conditions. In addition, to maximize rapid diffusion in the lithium layers, and thus battery performance, it is preferred to minimize the presence of metal elements in the lithium layers. It is further preferred that at least one of the metal elements be oxidizable within the electrochemical window of the electrolyte incorporated in the battery.

The cathode compositions may be synthesized by jet milling or by combining precursors of the metal elements (e.g., hydroxides, nitrates, and the like), followed by heating to generate the cathode composition. Heating is preferably conducted in air at temperatures of at least about 600°C, more preferably at least 800°C. In general, higher temperatures are

preferred because they lead to materials with increased crystallinity. The ability to conduct the heating process in air is desirable because it obviates the need and associated expense of maintaining an inert atmosphere. Accordingly, the particular metal elements are selected such that they exhibit appropriate oxidation states in air at the desired synthesis temperature.

Conversely, the synthesis temperature may be adjusted so that a particular metal element exists in a desired oxidation state in air at that temperature.

In general, examples of suitable metal elements for inclusion in the cathode composition include Ni, Co, Fe, Cu, Li, Zn, V, and combinations thereof. Particularly preferred cathode compositions are those having the following formulae:



The cathode compositions are combined with an anode and an electrolyte to form a lithium-ion battery. Examples of suitable anodes include lithium metal, graphite, and lithium alloy compositions, e.g., of the type described in Turner, U.S. 6,203,944 entitled "Electrode for a Lithium Battery" and Turner, WO 00/03444 entitled "Electrode Material and Compositions." The electrolyte may be liquid or solid. Examples of solid electrolytes include polymeric electrolytes such as polyethylene oxide, polytetrafluoroethylene, fluorine-containing copolymers, and combinations thereof. Examples of liquid electrolytes include ethylene carbonate, diethyl carbonate, propylene carbonate, and combinations thereof. The electrolyte is provided with a lithium electrolyte salt. Examples of suitable salts include LiPF_6 , LiBF_4 , and LiClO_4 .

The invention will now be described further by way of the following examples.

EXAMPLES

Electrochemical Cell Preparation

Electrodes were prepared as follows. About 21 wt. % active cathode material (prepared as described below), 5.3 wt. % Kynar Flex 2801 (a vinylidene fluoride-hexafluoropropylene copolymer commercially available from Atochem), 8.4 wt. % dibutyl phthalate, 2.1 wt. % Super S carbon black (commercially available from MMM Carbon,

Belgium), and 63.2 wt. % acetone were mechanically shaken for 1-2 hours in a mixing vial to which a zirconia bead (8 mm diameter) had been added to form a uniform slurry. The slurry was then spread in a thin layer (about 150 micrometers thick) on a glass plate using a notch-bar spreader. After evaporating the acetone, the resulting film was peeled from the glass and a circular electrode measuring 1.3 cm in diameter was punched from the film using an electrode punch, after which the electrode was soaked in diethyl ether for about 10 minutes to remove dibutyl phthalate and to form pores in the electrode. The ether rinse was repeated two times. The electrodes were then dried at 90°C overnight. At the conclusion of the drying period, the circular electrode was weighed and the active mass (the total weight of the circular electrode multiplied by the fraction of the electrode weight made up of the active cathode material) determined. Typically, the electrodes contained 74% by weight active material. The electrodes were then taken into an argon-filled glove box where the electrochemical cell was constructed.

An exploded perspective view of the electrochemical cell 10 is shown in FIG. 1. A stainless steel cap 24 and special oxidation resistant case 26 contain the cell and serve as the negative and positive terminals respectively. The cathode 12 was the electrode prepared as described above. The anode 14 was a lithium foil having a thickness of 125 micrometers; the anode also functioned as a reference electrode. The cell featured 2325 coin-cell hardware, equipped with a spacer plate 18 (304 stainless steel) and a disc spring 16 (mild steel). The disc spring was selected so that a pressure of about 15 bar would be applied to each of the cell electrodes when the cell was crimped closed. The separator 20 was a Celgard #2502 microporous polypropylene film (Hoechst-Celanese), which had been wetted with a 1M solution of LiPF_6 dissolved in a 30:70 volume mixture of ethylene carbonate and diethyl carbonate (Mitsubishi Chemical). A gasket 27 was used as a seal and to separate the two terminals.

Elemental Analysis

Approximately 0.02 g of each sample was accurately weighed on a microbalance (to 1 μg) into a 50 mL glass class A volumetric flask. 2 mL hydrochloric acid and 1 mL nitric acid were then added to form a salt. Once the salt had dissolved, the solution was diluted to 50 mL with deionized water and the solution shaken to mix. This solution was diluted

further 10 times. Next, a 5 mL aliquot was removed with a glass class A volumetric pipet and diluted to 50 mL in a glass class A volumetric flask with 4 % HCl and 2 % nitric acid.

The diluted solution were analyzed on a Jarrell-Ash 61E ICP using standards of 0, 1, 3, 10, and 20 ppm Co, Ni, Mn, Li, and Na in 4 % HCl / 2% HNO₃. A 5 ppm standard of each element was used to monitor the stability of the calibration. All standards were prepared from a certified stock solution and with class A volumetric glassware. Prior to analysis of the elements, the injector tube of the ICP was cleaned to remove any deposits. All element calibration curves exhibited r^2 values in excess of 0.9999.

The analytical results were measured in weight percent. These values were then converted to atomic percent and then ultimately to a stoichiometry where the oxygen content had been normalized to a stoichiometry of 2.

Examples 1-6

Example 1 describes the synthesis of 0.1 mole of $\text{Li}[\text{Li}_{(1-2y)/3}\text{Ni}_y\text{Mn}_{(2-y)/3}]\text{O}_2$ where $y = 0.416$.

12.223 g of $\text{Ni}(\text{NO}_3)_2 \cdot 6\text{H}_2\text{O}$ (Aldrich Chemical Co.) and 13.307 g of $\text{Mn}(\text{NO}_3)_2 \cdot 4\text{H}_2\text{O}$ (Aldrich Chemical Co.) were dissolved in 30 mls of distilled water to form a transition metal solution. In a separate beaker, 9.575 g of $\text{LiOH} \cdot \text{H}_2\text{O}$ (FMC Corp.) was dissolved in 200 mls of distilled water. While stirring, the transition metal solution was added dropwise using a buret to the lithium hydroxide solution over a period of about 3 hours. This caused the co-precipitation of a Ni-Mn hydroxide and the formation of LiNO_3 (dissolved). The precipitate was recovered by filtration and washed repeatedly using vacuum filtration. It was then placed in a box furnace set to 180°C to dry, after which it was mixed with 4.445 g $\text{LiOH} \cdot \text{H}_2\text{O}$ in an autogrinder and pressed into a number of pellets, each weighing two grams.

The pellets were heated in air at 480°C for 3 hours, after which they were quenched to room temperature, combined, and re-ground into powder. New pellets were pressed and heated in air to 900°C for 3 hours. At the conclusion of the heating step, the pellets were quenched to room temperature and again ground to powder to yield the cathode material.

Elemental analysis of the cathode material revealed that the composition had the following stoichiometry: $\text{Li}[\text{Li}_{0.06}\text{Ni}_{0.393}\text{Mn}_{0.51}]\text{O}_2$, which is in close agreement with the target stoichiometry of $\text{Li}[\text{Li}_{0.06}\text{Ni}_{0.42}\text{Mn}_{0.53}]\text{O}_2$.

Examples 2-6 were prepared in analogous fashion except that the relative amounts of reactants were adjusted to yield samples in which $y = 0.083$ (Example 2), 0.166 (Example 3), 0.25 (Example 4), 0.333 (Example 5), and 0.5 (Example 6). Elemental analysis of the cathode material from Example 5 revealed that the composition had the following stoichiometry: $\text{Li}[\text{Li}_{0.13}\text{Ni}_{0.314}\text{Mn}_{0.55}]\text{O}_2$, which is in close agreement with the target stoichiometry of $\text{Li}[\text{Li}_{0.11}\text{Ni}_{0.33}\text{Mn}_{0.56}]\text{O}_2$.

A powder x-ray diffraction pattern for each sample was collected using a Siemens D5000 diffractometer equipped with a copper target X-ray tube and a diffracted beam monochromator. Data was collected between scattering angles of 10 degrees and 130 degrees.

The crystal structure of each sample was determined based upon the x-ray diffraction data as described in (a) C. J. Howard and R. J. Hill, Australian Atomic Energy Commission Report No. M112 (1986); and (b) D. B. Wiles and R. A. Young, *J. Appl. Cryst.*, 14:149-151 (1981). Lattice parameters were determined using the Rietveld refinement. The lattice parameters for each sample are reported in Table 1. The crystal structure of each sample could be described well by the O3 crystal structure type.

Electrochemical cells were constructed according to the above-described procedure using the material of Examples 1 and 3-6 as the cathode. Each cell was charged and discharged between 4.4 V and 3.0 V at 30°C using computer-controlled discharge stations from Moli Energy Ltd. (Maple Ridge, B.C., Canada) and a current of 10 mA/g of active material. Fig. 3 is a plot of voltage versus capacity and capacity versus cycle number for each cell. Reversible and irreversible capacities were determined and are reported in Table 1. Each sample showed excellent reversibility and excellent capacity retention for at least 15 cycles.

A second set of electrochemical cells was constructed using the materials of Examples 1 and 3-6, and cycled as described above with the exception that the cells were charged and discharged between 4.8 V and 2.0 V using a current of 5 mA/g of active material. Fig. 3 is a plot of voltage versus capacity and capacity versus cycle number for each cell. Reversible and irreversible capacities were determined and are reported in Table 1. Each sample performed well. Examples 3 and 4 show large irreversible capacities, but still give stable reversible capacities over 200 mAh/g. Samples 1, 5, and 6 show irreversible

capacities less than 30 mAh/g and reversible capacities greater than 200 mAh/g. In particular, Example 1 shows an irreversible capacity of only about 15 mAh/g and a reversible capacity of about 230 mAh/g.

TABLE 1

Example	y	HTT (°C)	a (Å)	c (Å)	Rev. Capacity mAh/g 3.0-4.4V	Irrev. Capacity mAh/g 3.0-4.4V	Rev. Capacity mAh/g 2.0-4.8V	Irrev. Capacity mAh/g 2.0-4.8V
1	0.416	900	2.8793	14.2871	160	10	230	15
2	0.083	900	2.8499	14.2386	*	*	*	*
3	0.166	900	2.8589	14.2427	82	10	230	120
4	0.25	900	2.8673	14.258	117	12	250	50
5	0.333	900	2.8697	14.2654	142	10	240	25
6	0.5	900	2.8900	14.2971	140	10	200	25

“HTT” refers to the heat treatment temperature. “a” and “c” represent lattice parameters. An asterisk means “not tested.”

Another electrochemical cell was assembled using the material of Example 1 and cycled between 3.0 V and 4.4 V using a current of 30 mA/g. Some cycles were collected at 30°C, while other cycles were collected at 55°C. The results are reported in Fig. 12. The capacity of the material was maintained even at 55°C after extended cycling, demonstrating that the material did not exhibit phase separation after extended cycling.

Another electrochemical cell was assembled using the material of Example 1 and used to test the rate capability of the material. Data was collected at 30°C up to a 2.0 V cutoff. The results are shown in Fig. 13. The results demonstrate that the capacity of the material was maintained even up to discharge currents as large as 400 mA/g.

Examples 7-9

Examples 7-9 were prepared following the procedure described for Examples 1-6 where $y = 0.166$ except that the samples were heated at 600°C (Example 7), 700°C (Example 8), and 800°C (Example 9), rather than 900°C. X-ray diffraction patterns for each sample were collected and are shown in Fig. 3, along with an x-ray diffraction pattern for Example 3 prepared at 900°C. The lattice parameters were also determined and are set forth in Table 2, along with the data for Example 3. The data demonstrate that as the heating temperature increases, the peak widths in the diffraction patterns become narrower, indicating increased crystallinity. All peaks can be understood based on the O3 crystal structure.

TABLE 2

Example	y	HTT (°C)	a (Å)	c (Å)
7	0.166	600	2.8653	14.1739
8	0.166	700	2.8614	14.2076
9	0.166	800	2.8597	14.2289
3	0.166	900	2.8589	14.2427

“HTT” refers to the heat treatment temperature. “a” and “c” represent lattice parameters.

Examples 10-12

Examples 10-12 were prepared following the procedure described for Examples 1-6 where $y = 0.333$ except that the samples were heated at 600°C (Example 10), 700°C (Example 11), and 800°C (Example 12), rather than 900°C. X-ray diffraction patterns for each sample were collected and are shown in Fig. 4, along with an x-ray diffraction pattern for Example 5 prepared at 900°C. The lattice parameters were also determined and are set forth in Table 3, along with the data for Example 5. The data demonstrate that as the heating temperature increases, the peak widths in the diffraction patterns become narrower, indicating increased crystallinity. All peaks can be understood based on the O3 crystal structure.

Electrochemical cells were constructed using material from Examples 10 and 12 as the cathode, as cycled as described above. The reversible and irreversible capacities are also reported in Table 3, along with data for Example 5. All samples performed well.

TABLE 3

Example	y	HTT (°C)	a (Å)	c (Å)	Rev. Capacity mAh/g 3.0-4.4V	Irrev. Capacity mAh/g 3.0-4.4V	Rev. Capacity mAh/g 2.0-4.8V	Irrev. Capacity mAh/g 2.0-4.8V
10	0.333	600	2.8800	14.2389	110	50	210	65
11	0.333	700	2.8761	14.2569	*	*	*	*
12	0.333	800	2.8714	14.2644	120	20	230	50
5	0.333	900	2.8697	14.2654	160	10	230	15

“HTT” refers to the heat treatment temperature. “a” and “c” represent lattice parameters. An asterisk means “not tested.”

Examples 13-15

Examples 13-15 were prepared following the procedure described for Examples 1-6 where $y = 0.416$ except that the samples were heated at 600°C (Example 13), 700°C (Example 14), and 800°C (Example 15), rather than 900°C. The lattice parameters were determined for each sample and are set forth in Table 4, along with the data for Example 1 ($y = 0.416$, 900°C). These samples also exhibited the O3 crystal structure.

TABLE 4

Example	y	HTT (°C)	a (Å)	c (Å)
13	0.416	600	2.8829	14.2609
14	0.416	700	2.8824	14.2720
15	0.416	800	2.8824	14.2808
1	0.416	900	2.8793	14.2781

“HTT” refers to the heat treatment temperature. “a” and “c” represent lattice parameters.

Examples 16-18

Examples 16-18 were prepared following the procedure described for Examples 1-6 where $y = 0.5$ except that the samples were heated at 600°C (Example 16), 700°C (Example 17), and 800°C (Example 18), rather than 900°C. X-ray diffraction patterns for each sample were collected and are shown in Fig. 6, along with an x-ray diffraction pattern for Example 6 prepared at 900°C. The lattice parameters were also determined and are set forth in Table 5, along with the data for Example 6. The data demonstrate that as the heating temperature increases, the peak widths in the diffraction patterns become narrower, indicating increased crystallinity. All peaks can be understood based on the O3 crystal structure.

Electrochemical cells were constructed using material from Examples 16-18 as the cathode, as cycled as described above. The reversible and irreversible capacities are also reported in Table 5, along with data for Example 6. In addition, Fig. 7 reports voltage versus capacity and capacity versus cycle number for each cell, as well as a cell constructed using Example 6, when cycled between 4.4 V and 3.0 V. Fig. 8 reports voltage versus capacity and capacity versus cycle number for each cell, as well as a cell constructed using Example 6, when cycled between 4.8 V and 2.0 V. All samples performed well, with samples prepared at higher temperatures exhibiting the best capacity retention and lowest irreversible capacity.

TABLE 5

Example	y	HTT (°C)	a (Å)	c (Å)	Rev. Capacity mAh/g 3.0-4.4V	Irrev. Capacity mAh/g 3.0-4.4V	Rev. Capacity mAh/g 2.0-4.8V	Irrev. Capacity mAh/g 2.0-4.8V
16	0.5	600	2.8926	14.298	120	60	200	50
17	0.5	700	2.8914	14.2842	140	20	210	25
18	0.5	800	2.8889	14.2812	145	15	210	20
6	0.5	900	2.8899	14.2964	140	10	200	25

“HTT” refers to the heat treatment temperature. “a” and “c” represent lattice parameters.

Examples 19-20

Example 19 describes the preparation of 0.1 mole of $\text{Li}[\text{Ni}_y\text{Co}_{1-2y}\text{Mn}_y]\text{O}_2$ where $y = 0.375$. The procedure described in Examples 1-6 was followed except that the following reactants were used: 10.918 g of $\text{Ni}(\text{NO}_3)_2 \cdot 6\text{H}_2\text{O}$, 9.420 g of $\text{Mn}(\text{NO}_3)_2 \cdot 4\text{H}_2\text{O}$, and 7.280 g of $\text{Co}(\text{NO}_3)_2 \cdot 6\text{H}_2\text{O}$. In addition, the dried transition metal hydroxide was mixed with 4.195 g of $\text{LiOH} \cdot \text{H}_2\text{O}$. The lattice parameters were measured and determined to be: $a = 2.870 \text{ \AA}$ and $c = 14.263 \text{ \AA}$. Elemental analysis of the material revealed that the composition had the following stoichiometry: $\text{Li}_{1.04}[\text{Ni}_{0.368}\text{Co}_{0.263}\text{Mn}_{0.38}]\text{O}_2$, which is in close agreement with the target stoichiometry of $\text{Li}[\text{Ni}_{0.375}\text{Co}_{0.25}\text{Mn}_{0.375}]\text{O}_2$.

Example 20 was prepared in similar fashion except that the relative amounts of ingredients were adjusted to yield $y = 0.25$. The lattice parameters were measured and determined to be: $a = 2.8508$ and $c = 14.206 \text{ \AA}$. Elemental analysis of the material revealed that the composition had the following stoichiometry: $\text{Li}_{1.03}[\text{Ni}_{0.243}\text{Co}_{0.517}\text{Mn}_{0.25}]\text{O}_2$, which is in close agreement with the target stoichiometry of $\text{Li}[\text{Ni}_{0.25}\text{Co}_{0.5}\text{Mn}_{0.25}]\text{O}_2$.

Electrochemical cells were constructed using material from Examples 19-20 as the cathode, as cycled as described above. Fig. 9 reports voltage versus capacity for each cell when cycled between 2.5 V and 4.8 V. Both samples performed well.

A second set of electrochemical cells was constructed using material from Examples 19-20 and cycled as described above between 2.5 V and 4.4 V using a current of 40 mA/g. The results are shown in Figs. 10 and 11. In the case of Example 19 (Fig. 10), data was collected at both 30°C and 55°C, whereas in the case of Example 20 (Fig. 11) data was collected at 30°C only. Both samples performed well.

The cathode material from Example 19 was further analyzed using differential scanning calorimetry (DSC). The sample cell was a 3.14 mm outer diameter, type 304 stainless steel seamless tube having a wall thickness of 0.015 mm that had been cut into an 8.8 mm long piece (MicroGroup, Medway, MA). The cell was cleaned, after which one end

was flattened. The flattened end was then welded shut by tungsten inert gas welding using a Miller Maxstar 91 ARC welder equipped with a Snap Start II high frequency ARC starter.

Once the flattened end had been sealed, the tube was loaded in an argon-filled glove box with 2 mg of the cathode material from Example 19 taken from a 2325 coin cell that had been charged to 4.2 V using the procedure described above. The electrolyte was not removed from the cathode sample. After the sample was loaded, the tube was crimped and welded shut.

The DSC measurements were performed using a TA Instruments DSC 910 instrument. The DSC sweep rate was 2°C/minute. Both the onset temperature and the total heat evolved were recorded. The onset temperature corresponds to the temperature at which the first major exothermic peak occurs. The results are shown in Table 6. For the sake of comparison, data from cathodes prepared using LiNiO₂ and LiCoO₂ is included as well. The results demonstrate that cathodes prepared using the material from Example 19 exhibited a higher onset temperature and evolved less heat than cathodes prepared using LiNiO₂ and LiCoO₂.

TABLE 6

Material	Onset Temperature (°C)	Total Heat (J/g)
Example 19	290	404
LiNiO ₂	180	1369
LiCoO ₂	185	701

A number of embodiments of the invention have been described. Nevertheless, it will be understood that various modifications may be made without departing from the spirit and scope of the invention. Accordingly, other embodiments are within the scope of the following claims.